J|A|C|S
ARTICLES

Published on Web 05/03/2010

Selectivity Principles in Anion Separation by Crystallization of Hydrogen-Bonding Capsules

Radu Custelcean,* Aurelien Bock, and Bruce A. Moyer

Chemical Sciences Division, Oak Ridge National Laboratory, Oak Ridge, Tennessee 37831

Received February 15, 2010; E-mail: custelceanr@ornl.gov

Abstract: The fundamental factors controlling anion selectivity in the crystallization of hydrogen-bonding capsules $[Mg(H_2O)_6][X \subset \mathbf{L}_2]$ ($X = SO_4^{2-}$, **1a**; SeO_4^{2-}, **1b**; SO_3^{2-}, **1c**; CO_3^{2-}, **1d**; **L** = tris[2-(3-pyridylurea)ethyl]-amine) from water have been investigated by solution and solid-state thermodynamic measurements, anion competition experiments, and X-ray structural analysis. The crystal structures of **1a**−**d** are isomorphous, thereby simplifying the interpretation of the observed selectivities based on differences in anion coordination geometries. The solubilities of **1a**−**d** in water follow the order: **1a** < **1b** < **1c** < **1d**, which is consistent with the selectivity for the tetrahedral sulfate and selenate anions observed in competitive crystallization experiments. Crystallization of the capsules is highly exothermic, with the most favorable ΔH°_{cryst} of −99.1 and −108.5 kJ/mol corresponding to SO_4^{2-} and SeO_4^{2-}, respectively, in agreement with the X-ray structural data showing shape complementarity between these tetrahedral anions and the urea-lined cavities of the capsules. Sulfite, on the other hand, has a significantly less negative ΔH°_{cryst} of −64.6 kJ/mol, which may be attributed to its poor fit inside the capsules, involving repulsive interactions. The more favorable entropy of crystallization for this anion, however, partly offsets the enthalpic disadvantage, resulting in a solubility product very similar to that of the selenate complex. Because of their very similar shape and size, SO_4^{2-} and SeO_4^{2-} have a propensity to form solid solutions, which limits the selectivity between these two anions in competitive crystallizations. In the end, a comprehensive picture of contributing factors to anion selectivity in crystalline hydrogen-bonding capsules emerges.

Introduction

Following the first report of anion complexation by a protonated macrobicyclic diamine ligand in 1968 by Park and Simmons,[1] anion coordination chemistry[2,3] has become a rich and vibrant area of research, developing into a distinct branch of supramolecular chemistry. After more than 40 years of research in this field, however, examples of size- and shape-selective anion receptors that work effectively in competitive aqueous environments remain rare.[4,5] As recognized early on by Lehn et al., exceptional binding strength and selectivity can be achieved by completely isolating the anion from the surrounding solvent via encapsulation inside rigid three-dimensional hosts possessing cavities lined with appropriate binding groups that are geometrically constrained to prevent effective binding of competing anions.[6] These concepts, though simple in principle, remain difficult to apply in practice, as the synthesis of three-dimensional cryptand-like hosts internally functionalized with appropriate binding groups is labor intensive and inefficient. Even when successfully synthesized, such hosts are rarely rigid enough to prevent structural distortions that allow accommodation of competing guests. Furthermore, small anions have relatively high free energies of hydration and resultant binding and partitioning behavior that follows a monotonous trend (Hofmeister bias) defining a selectivity baseline that is difficult to overcome.[3c] For the same reason, complete stripping of the anions' hydration shells may not be possible in some cases, resulting in reduced binding strengths and selectivities. Despite all these difficulties, some remarkable examples of anion encapsulation by synthetic receptors from aqueous environments have been reported.[4−6] Highly protonated polyammonium and metal-containing cage receptors have proven particularly useful for this purpose.[7] One challenge associated with highly charged receptors in water is that their anion binding is often thermo-

(1) Park, C. H.; Simmons, H. E. *J. Am. Chem. Soc.* **1968**, *90*, 2431.
(2) Sessler, J. L.; Gale, P. A.; Cho, W. S. *Anion Receptor Chemistry, Monographs in Supramolecular Chemistry*; Stoddart, J. F., Ed.; Royal Society of Chemistry: Cambridge, 2006.
(3) (a) Caltagirone, C.; Gale, P. A. *Chem. Soc. Rev.* **2009**, *38*, 520. (b) Gale, P. A.; Garcia-Garrido, S. E.; Garric, J. *Chem. Soc. Rev.* **2008**, *37*, 151. (c) Custelcean, R.; Moyer, B. A. *Eur. J. Inorg. Chem.* **2007**, *10*, 1321. (d) Arnendola, V.; Bonizzoni, M.; Esteban-Gomez, D.; Fabbrizzi, L.; Licchelli, M.; Sancenon, F.; Taglietti, A. *Coord. Chem. Rev.* **2006**, *250*, 1451. (e) Bowman-James, K. *Acc. Chem. Res.* **2005**, *38*, 671. (f) F. P. Schmidtchen, F. P.; Berger, M. *Chem. Rev.* **1997**, *97*, 1609.
(4) (a) Schmidtchen, F. P. *Angew. Chem., Int. Ed.* **1977**, *89*, 751. (b) Lehn, J.-M.; Sonveaux, E.; Willard, A. K. *J. Am. Chem. Soc.* **1978**, *100*, 4914. (c) Fabbrizzi, L.; Faravelli, I.; Francese, G.; Licchelli, M.; Perotti, A.; Taglietti, A. *Chem. Commun.* **1998**, 971. (d) Fabbrizzi, L.; Leone, A.; Taglietti, A. *Angew. Chem., Int. Ed.* **2001**, *40*, 3066. (e) Kubik, S.; Kirchner, R.; Nolting, D.; Seidel, J. *J. Am. Chem. Soc.* **2002**, *124*, 12752. (f) Tobey, S. J.; Jones, B. D.; Anslyn, E. V. *J. Am. Chem. Soc.* **2003**, *125*, 4026. (g) Schmuck, C. *Coord. Chem. Rev.* **2006**, *250*, 3053. (h) Reyheller, C.; Kubik, S. *Org. Lett.* **2007**, *9*, 5271. (i) Hancock, L. M.; Beer, P. D. *Chem.—Eur. J.* **2009**, *15*, 42. (j) Custelcean, R.; Bosano, J.; Bonnesen, P. V.; Kertesz, V.; Hay, B. P. *Angew. Chem., Int. Ed.* **2009**, *48*, 4025.
(5) Kubik, S.; Reyheller, C.; Stuwe, S. *J. Inclusion Phenom. Macrocyclic Chem.* **2005**, *52*, 137.
(6) Graf, E.; Lehn, J.-M. *J. Am. Chem. Soc.* **1976**, *98*, 6403.

neutral or even endothermic, and thereby entropy driven,[5,7b] making their molecular design and prediction of anion affinity difficult.

We and others have recently demonstrated an alternative approach to traditional anion binding in solution, based on selective inclusion of anions into crystalline frameworks.[8,9] This process consists of competitive crystallization of organic salts, or cocrystallization of inorganic salts with neutral organic ligands, where high anion selectivity may be achieved by functionalization of the organic components with strong and specific anion-binding groups. In many ways, the impetus for this work derives from over a century of coordination chemistry in solution, first of cations and more recently of anions. In such work, crystallization has traditionally been a route to understanding the structure of the complexes formed, primarily by X-ray crystallography. Structural insights are then related to the observed selectivity in solution. Despite well-known pitfalls,[10] cautious correlation of solid-state structures with solution phenomena has proven extremely helpful. Now, we are exploring the possibility of using crystallization not only with the purpose of obtaining structural insights into anion binding in solution, but also as a means for selective anion separation. Though ion separation by crystallization of simple inorganic salts has long been exploited as a classical technique, it offers limited control over selectivity through matching of the relative size of the counterions.[11] In contrast, organic crystals offer the prospect of designed selectivity through introduction of molecular recognition elements, much in the same way as in classical molecular receptors. It should be noted here, though, that typically crystals will not act as hosts in the traditional sense, as they generally cannot stand alone in the absence of the 'guest' ions, which may be integral components of the crystalline assemblies. Nevertheless, parallels can be drawn to host−guest chemistry in solution, since the ionic and molecular components also need to be desolvated before they assemble into the crystalline framework. However, the ensuing host−guest environment in a crystal is determined not so much by the influence of external solvent molecules, but rather by the constraints of the lattice and packing forces. As a result, it is expected that the selectivity observed in crystallization will not strictly follow the selectivity of complexation in solution. The stiffer environment found in a crystal may in fact provide better organizational rigidity,[3c] thereby preventing the accommodation of undesired competing anions through structural distortions and rearrangements of the host framework. Under ideal circumstances, when no alternative crystal structures that can accommodate competing anions are possible, the excluded anions may in principle be rejected with infinite selectivity, giving crystallization a unique advantage over other separation techniques.

When interpreting anion selectivity in competitive crystallizations, it is convenient to analyze series of isomorphous crystals (same space group and crystal packing, and similar lattice parameters), where the observed trends may be directly attributed to differences in anion coordination obtained by X-ray diffraction. However, such isomorphous series are rare, as various anions with different shapes and charge densities tend to form completely different crystal structures. In such cases, the rationalization of the observed selectivities becomes a difficult exercise, as other factors, such as packing efficiency, dimensionality of the framework, and nature of the exposed groups on crystal surfaces may determine relative solubilities and thus anion selectivities.[8g]

One series of isomorphous anion-coordinating crystals was recently discovered in our laboratory[8e] using a simple tripodal tris(3-pyridylurea) ligand **L** (**L** = tris[2-(3-pyridylurea)ethyl]-amine) that combines the tren structural scaffold[12] with urea anion-binding groups,[13] both common elements in the design of molecular receptors. The pyridine end groups were added for incorporation into extended frameworks through cation coordination. **L** self-assembles from water/methanol solutions in the presence of Mg^{2+} and divalent oxoanions like sulfate, selenate, sulfite, and carbonate, into crystalline capsules with the formula $[Mg(H_2O)_6][X\subset\mathbf{L}_2]$ (X = SO_4^{2-}, **1a**; SeO_4^{2-}, **1b**; SO_3^{2-}, **1c**; CO_3^{2-}, **1d**), connected into three-dimensional hydrogen-bonded frameworks through bridging $Mg(H_2O)_6^{2+}$ cations (Figure 1).[14] Like other analogous tren-urea derivatives, **L** provides a highly complementary environment for the tetrahedral sulfate anion, encapsulating it by 12 hydrogen bonds in a 2:1 complex in the solid state.[15] According to electronic-structure calculations, this represents the ideal coordination number for SO_4^{2-}.[16] More notable though was the fact that, despite its very flexible nature, **L** self-assembled into virtually identical crystalline capsules with the larger selenate, or the

(7) (a) Llinares, J. M.; Powell, D.; Bowman-James, K. *Coord. Chem. Rev.* **2003**, *240*, 57. (b) Garcia-Espana, E.; Diaz, P.; Llinares, J. M.; Bianchi, A. *Coord. Chem. Rev.* **2006**, *250*, 2952. (c) McKee, V.; Nelson, J.; Town, R. M. *Chem. Soc. Rev.* **2003**, *32*, 309. (d) Amendola, V.; Fabbrizzi, L.; Mangano, C.; Pallavicini, P.; Poggi, A.; Taglietti, A. *Coord. Chem. Rev.* **2001**, *219*−*221*, 821. (e) Amendola, V.; Fabbrizzi, L. *Chem. Commun.* **2009**, 513.

(8) (a) Custelcean, R.; Gorbunova, M. G. *J. Am. Chem. Soc.* **2005**, *127*, 16362. (b) Custelcean, R.; Haverlock, T. J.; Moyer, B. A. *Inorg. Chem.* **2006**, *45*, 6446. (c) Custelcean, R.; Sellin, V. *Chem. Commun.* **2007**, 1541. (d) Custelcean, R.; Jiang, D. E.; Hay, B. P.; Luo, W.; Gu, B. *Cryst. Growth Des.* **2008**, *8*, 1909. (e) Custelcean, R.; Remy, P.; Bonnesen, P. V.; Jiang, D. E.; Moyer, B. A. *Angew. Chem., Int. Ed.* **2008**, *47*, 1866. (f) Custelcean, R.; Remy, P. *Cryst. Growth. Des.* **2009**, *9*, 1985. (g) Custelcean, R. *Curr. Opin. Solid State Mater. Sci.* **2009**, *13*, 68.

(9) (a) Wu, B.; Huang, X.; Xia, Y.; Yang, X. J.; Janiak, C. *CrystEngComm* **2007**, *9*, 676. (b) Uzarevic, K.; Dilovic, I.; Matkovic-Calogovic, D.; Sisak, D.; Cindric, M. *Angew. Chem., Int. Ed.* **2008**, *47*, 7022. (c) Adarsh, N. N.; Kumar, D. K.; Dastidar, P. *CrystEngComm* **2008**, *10*, 1565. (d) Adarsh, N. N.; Kumar, D. K.; Dastidar, P. *CrystEngComm* **2009**, *11*, 796. (e) Xia, Y.; Wu, B.; Liu, Y.; Yang, Z.; Huang, X.; He, L.; Yang, X. J. *CrystEngComm* **2009**, *11*, 1849. (f) Zhuge, F.; Wu, B.; Liang, J.; Yang, J.; Liu, Y.; Jia, C.; Janiak, C.; Tang, N.; Yang, X. J. *Inorg. Chem.* **2009**, *48*, 10249.

(10) Schmidtchen, F. P. *Coord. Chem. Rev.* **2006**, *250*, 2918.

(11) J. E. Huheey, J. E. *Inorganic Chemistry: Principles of Structure and Reactivity*; Harper & Row: New York, 1972.

(12) Bazzicalupi, C.; Bencini, A.; Bianchi, A.; Danesi, A.; Giorgi, C.; Valtancoli, B. *Inorg. Chem.* **2009**, *48*, 2391, and references therein.

(13) (a) Clare, J. P.; Statnikov, A.; Lynch, V.; Sargent, A. L.; Sibert, J. W. *J. Org. Chem.* **2009**, *74*, 6637. (b) Meshcheryakov, D.; Bohmer, V.; Bolte, M.; M. Hubscher-Bruder, M.; Arnaud-Neu, F. *Chem.*−*Eur. J.* **2009**, *15*, 4811. (c) Warr, R. J.; Westra, A. N.; Bell, K. J.; Chartres, J.; Ellis, J. R.; Tong, C.; Simmance, T. G.; Gadzhieva, A.; Blake, A. J.; Tasker, P. A.; Schroder, M. *Chem.*−*Eur. J.* **2009**, *15*, 4836. (d) McNally, B. A.; O'Neil, E. J.; Nguyen, A.; Smith, B. D. *J. Am. Chem. Soc.* **2008**, *130*, 17274. (e) dos Santos, C. M. G.; McCabe, T.; Watson, G. W.; Kruger, P. E.; Gunnlaugsson, T. *J. Org. Chem.* **2008**, *73*, 9235. (f) Caltagirone, C.; Hiscock, J. R.; Hursthouse, M. B.; Light, M. E.; Gale, P. A. *Chem.*−*Eur. J.* **2008**, *14*, 10236–10243. (g) Allevi, M.; Bonizzoni, M.; Fabbrizzi, L. *Chem.*−*Eur. J.* **2007**, *13*, 3787. (h) Turner, D. R.; Paterson, M. J.; Steed, J. W. *J. Org. Chem.* **2006**, *71*, 1598.

(14) Isomorphous crystals can be obtained from Zn^{2+}, Cd^{2+}, Co^{2+},[8e] or Mn^{2+}: (a) Wu, B.; Liang, J.; Yang, J.; Jia, C.; Yang, X. J.; Zhang, H.; Tang, N.; Janiak, C. *Chem. Commun.* **2008**, 1762.

(15) (a) Custelcean, R.; Moyer, B. A.; Hay, B. P. *Chem. Commun.* **2005**, 5971. (b) Ravikumar, I.; Lakshminarayanan, P. S.; Arunachalam, M.; Suresh, E.; Ghosh, P. *Dalton. Trans.* **2009**, 4160.

(16) Hay, B. P.; Firman, T. K.; Moyer, B. A. *J. Am. Chem. Soc.* **2005**, *127*, 1810.

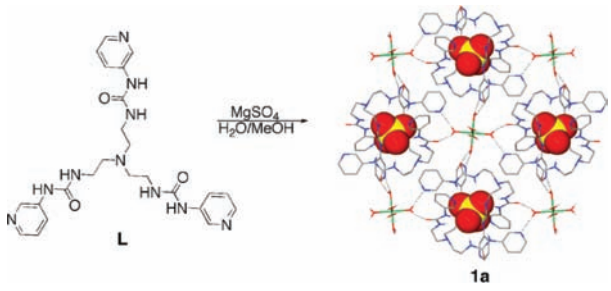

Figure 1. Self-assembly of the prototype crystalline framework **1a**, consisting of $SO_4(\mathbf{L})_2^{2-}$ capsules connected into a hydrogen-bonded framework by $Mg(H_2O)_6^{2+}$.[8e]

differently shaped sulfite and carbonate, with minimal conformational distortions. We attributed this remarkable structural persistence to the hydrogen-bonding $Mg(H_2O)_6^{2+}$ cationic bridges that substantially rigidify the capsules in the solid state, helping them retain their shape. Crystal structure analyses showed that while the urea-lined cavities of the capsules were a good match with the tetrahedral SO_4^{2-} and SeO_4^{2-}, the pyramidal SO_3^{2-} and the trigonal-planar CO_3^{2-} did not fit so well, engaging in repulsive NH···S and NH···C interactions. Preliminary competitive crystallization experiments in H_2O/MeOH yielded the following selectivity trend: $SO_4^{2-} > SeO_4^{2-} \gg CO_3^{2-} > SO_3^{2-}$, consistent with the structural observations.[8e] However, a number of questions remained unanswered: (1) Do the hydrogen-bonded capsules persist in solution? (2) To what extent was the observed selectivity the result of thermodynamics versus kinetics? (3) Do the relative solubilities of **1a**−**d** correlate with the observed anion selectivity in competitive crystallizations? (4) What are the enthalpic and entropic contributions to the crystallization of the capsules? and (5) Does shape recognition really determine selectivity, and how is shape complementarity reflected in the thermodynamic parameters? This paper will address these questions based on solution and solid-state thermodynamic measurements, anion competition experiments, and structural analysis, with the goal of elucidating the basic principles of selectivity for anion encapsulation in crystalline hydrogen-bonding capsules.

Experimental Section

Ligand **L** was synthesized as previously reported[8e] and recrystallized from EtOH−H_2O 1:4 (v/v) prior to use. The $MgX(\mathbf{L})_2(H_2O)_6$ crystals **1a**−**d** (X = SO_4^{2-}, SeO_4^{2-}, SO_3^{2-}, CO_3^{2-}) were prepared according to the previously published procedures,[8e] and their phase purity was confirmed by powder X-ray diffraction. FT-IR spectra were recorded in KBr pellets with a Digilab FTS 7000 spectrometer. Elemental analyses were performed by Galbraith Laboratories, Inc.

Potentiometric titrations were performed with an automated Mettler DL77 titrator controlled by LabX light V2.6 software. The pH glass electrode was calibrated prior to use by a standard titration of NaOH with HCl. All titrations were carried out at 25 (±1) °C under an Ar atmosphere. In a typical experiment, 42 mL of a solution containing **L** (0.75 mM), HNO_3 (3 mM), and KNO_3 electrolyte (75 mM) was titrated with a 0.1 M solution of NaOH that was previously standardized against phthalic acid (15 mM). Each recorded equivalence point was the average of at least three titrations. The titration data were modeled with Hyperquad 2006.[17]

Inductively Coupled Plasma (ICP) measurements were performed with an IRIS Intrepid II XPS optical emission spectrometer by analyzing the 279.55 nm wavelength of magnesium. Concentrations of Mg^{2+} ion were determined using a calibration curve obtained with standard solutions with concentrations ranging between 0.1 and 5 ppm obtained from a high-purity Mg^{2+} standard (1000 ± 0.3 ppm).

Determination of Solubility Product of 1a by Potentiometric Titrations. To suspensions of **1a** (30 mg) in 15 mL of KNO_3 electrolyte solutions (75 mM) were added increasing amounts of HNO_3 (between 1 and 3 equiv relative to **1a**). The mixtures were stirred overnight at 25 °C in an incubator, then the pH of the saturated solutions were measured with the glass electrode. Following filtration on a Millipore filter paper (0.45 μm), an excess of HNO_3 was added to each filtrate to completely protonate the dissolved ligand. The total content of $\mathbf{L}H_n^{n+}$ species was then determined by titration with NaOH. The concentrations of free ligand **L** required to calculate the K_{sp} were then determined based on the measured pH values of the saturated solutions and the previously measured protonation constants of **L**. The corresponding concentrations of free Mg^{2+} and SO_4^{2-} were derived from the known stoichiometry of **1a** and the measured equilibrium constants for sulfate binding by $\mathbf{L}H_n^{n+}$ in water. [Mg^{2+}] was also measured independently by ICP.

Determination of Solubility Product of 1a by ICP. Saturated solutions of **1a** in the presence of increasing amounts of sulfate were obtained by mixing 20 mg of the crystalline complex with K_2SO_4 (0−500 molar equiv) and 30 mg of $Na_2B_4O_7 \cdot 10H_2O$ (borax) in 15 mL of water that was previously boiled to remove the CO_2. The measured pH values of the solutions were between 9.35 and 9.37. The mixtures were mechanically stirred in an incubator for 5 days, and the resulting suspensions were filtered through syringe filters (IC Acrodisc with 0.2 μm PES membrane), discarding the first 20 drops of solution. The filtrates were acidified with conc. HNO_3 to reach a concentration of 1% in acid, then were subjected to ICP analyses. The Mg^{2+} concentrations were recorded as the average of at least four separate measurements.

Determination of Solubility Products of 1b−c by ICP. Saturated solutions of **1b** and **1c** were obtained by mixing 20 mg of each crystalline complex with 5−10 mg of borax in 15 mL of water that was previously boiled to remove the CO_2. The measured pH values of the solutions were 9.35−9.37. The mixtures were mechanically stirred in an incubator for 5 days, and the resulting suspensions were filtered through syringe filters (IC Acrodisc with 0.2 μm PES membrane), discarding the first 20 drops of solution. The filtrates were acidified with conc. HNO_3 to reach a concentration of 1% in acid, then were subjected to ICP analyses. The Mg^{2+} concentrations were recorded as the average of at least four separate measurements. The calculated K_{sp} were the average values obtained from 5−6 independent dissolution experiments.

Competitive Crystallization Experiments. (*A*) To a solution of **L** (101 mg, 0.2 mmol), HNO_3 (0.6 mmol), $Mg(NO_3)_2$ (0.1 mmol), and borax (0.381 g, 1 mmol) in 75 mL water was added 0.1 mmol each of Na_2SO_4, Na_2SeO_4, Na_2SO_3, and Na_2CO_3. The solution was stirred under Ar at room temperature for 5 days. The resulting precipitate was filtered and washed with water and MeOH. Yield 90 mg.

(*B*) To a solution of **L** (101 mg, 0.2 mmol), HNO_3 (0.6 mmol), and $Mg(NO_3)_2$ (0.1 mmol) in 75 mL water was added 0.1 mmol each of Na_2SO_4 and Na_2SeO_4. The solution was buffered with borax (0.381 g, 1 mmol), and stirred under Ar at room temperature for 5 days. The resulting precipitate was filtered and washed with water and MeOH. Yield 99 mg. Elemental analysis: SO_4^{2-}/SeO_4^{2-} (mol/mol) = 2.7.

(*C*) To a solution of **L** (101 mg, 0.2 mmol), HNO_3 (0.6 mmol), and $Mg(NO_3)_2$ (0.1 mmol) in 75 mL water was added 0.1 mmol of Na_2SO_4. The solution was buffered with borax (0.381 g, 1 mmol), and stirred under Ar at room temperature for 14 h, which resulted in the precipitation of **1a**. Na_2SeO_4 (0.1 mmol) was subsequently added, and the suspension was stirred at room temperature for 5 days. The resulting precipitate was filtered and washed with water and MeOH. Yield 97 mg. Elemental analysis: SO_4^{2-}/SeO_4^{2-} (mol/mol) = 2.4.

(17) Gans, P.; Sabatini, A.; Vacca, A. *Talanta* **1996**, *43*, 1739.

Table 1. Crystallographic Data for $\mathbf{L}H_4(SO_4)_2$ and $\mathbf{1a}_x\mathbf{b}_{1-x}$

	$LH_4(SO_4)_2$	$1a_{0.35}b_{0.65}$	$1a_{0.52}b_{0.48}$	$1a_{0.57}b_{0.43}$
formula	$C_{24}H_{34}N_{10}O_{16.5}S_2$	$C_{48}H_{72}MgN_{20}O_{16}S_{0.35}Se_{0.65}$	$C_{48}H_{72}MgN_{20}O_{16}S_{0.52}Se_{0.48}$	$C_{48}H_{72}MgN_{20}O_{16}S_{0.57}Se_{0.43}$
M	790.73	1272.11	1264.14	1261.79
cryst size (mm^3)	0.24 × 0.21 × 0.14	0.14 × 0.13 × 0.10	0.16 × 0.15 × 0.06	0.16 × 0.16 × 0.07
cryst syst	monoclinic	monoclinic	monoclinic	monoclinic
space group	$P2_1/c$	$P2_1/n$	$P2_1/n$	$P2_1/n$
a (Å)	18.4727(13)	12.4707(8)	12.4720(8)	12.4742(8)
b (Å)	14.7923(10)	18.3638(11)	18.3585(11)	18.3503(11)
c (Å)	13.2274(9)	13.0812(8)	13.0580(8)	13.0549(8)
β (deg)	105.85(10)	91.486(1)	91.490(1)	91.540(1)
V ($Å^3$)	3477.0(4)	2994.7(3)	2988.8(3)	2987.3(3)
Z	4	2	2	2
T (K)	173(1)	173(1)	173(1)	173(1)
ρ_{calcd} (g cm^{-3})	1.511	1.411	1.405	1.403
$2\theta_{max}$ (deg)	56.68	56.66	56.68	56.58
μ (cm^{-1})	0.241	0.520	0.423	0.395
reflns collected	35527	34321	36283	33941
ind reflns	8662	7470	7454	7426
parameters	482	434	434	434
R_{int}	0.0388	0.0383	0.0427	0.0437
R_1,[a] wR_2[b] ($I > 2\sigma(I)$)	0.0873, 0.2547	0.0387, 0.0920	0.0421, 0.0947	0.0434, 0.0944
GOF	1.086	1.028	1.043	1.029

[a] $R_1 = \sum(|F_0| - |F_c|)/\sum|F_0|$. [b] $wR_2 = \{\sum[w(F_0^2 - F_c^2)^2]/\sum[w(F_0^2)^2]\}^{1/2}$.

(*D*) To a solution of **L** (101 mg, 0.2 mmol), HNO_3 (0.6 mmol), and $Mg(NO_3)_2$ (0.1 mmol) in 75 mL water was added 0.1 mmol of Na_2SeO_4. The solution was buffered with borax (0.381 g, 1 mmol), and stirred under Ar at room temperature for 14 h, which resulted in the precipitation of **1b**. Na_2SO_4 (0.1 mmol) was subsequently added, and the suspension was stirred at room temperature for 5 days. The resulting precipitate was filtered and washed with water and MeOH. Yield 98 mg. Elemental analysis: SO_4^{2-}/SeO_4^{2-} (mol/mol) = 2.9.

X-ray Crystallography. Single crystals of $\mathbf{L}H_4(SO_4)_2(H_2O)_{5.5}$ were grown by slow evaporation of an ethanol solution containing **L** (0.1 mmol) and H_2SO_4 (0.05 mmol). Mixed $Mg(SO_4)_x(SeO_4)_{1-x}(\mathbf{L})_2(H_2O)_6$ ($\mathbf{1a}_x\mathbf{b}_{1-x}$) single crystals were grown by layering a methanol solution of **L** (0.2 mmol, 2 mL) over a 3 mL aqueous solution containing $Mg(NO_3)_2$ (0.1 mmol), Na_2SO_4 (0.1 mmol), and Na_2SeO_4 (0.1 mmol). Single crystals were collected at various intervals of times and analyzed by X-ray diffraction.

Single-crystal X-ray data were collected on a Bruker SMART APEX CCD diffractometer with fine-focus Mo Kα radiation (λ = 0.71073 Å), operated at 50 kV and 30 mA. The structures were solved by direct methods and refined on F^2 using the SHELXTL software package.[18] Absorption corrections were applied using SADABS, part of the SHELXTL package. All non-hydrogen atoms were refined anisotropically. Hydrogen atoms were placed in idealized positions and refined with a riding model. A summary of crystallographic data is listed in Table 1.

Results

Ion Binding in Solution. The binding of SO_4^{2-} and Mg^{2+} by **L** (in various protonation states) in water was investigated using potentiometric titrations, a very convenient method for determination of equilibrium constants involving ligands with multiple protonation states.[19] These measurements were done in order to account for all existing complexes in solution at various pH values, a prerequisite for the correct determination of the equilibrium constants associated with the precipitation of the final crystalline frameworks.

First, the pK_a values for the four protonation steps of **L**, corresponding to the three pyridine rings and the tertiary amine group, were measured. This could be easily done by completely protonating the ligand with a slight excess of nitric acid and back-titrating the $\mathbf{L}H_4^{4+}$ with NaOH. Although only two equivalent points are clearly visible, all four protonation constants could be unambiguously extracted from the titration curve by modeling the equilibria with Hyperquad (Supporting Information). The obtained pK_a values (in 75 mM KNO_3) for $\mathbf{L}H_n^{n+}$ are 3.58(1), 4.37(1), 5.23(1), and 7.11(1).

Next, the titration of $\mathbf{L}H_n^{n+}$ was repeated in the presence of 10-fold molar excess (relative to **L**) of Mg^{2+} or SO_4^{2-}, added as $Mg(NO_3)_2$ or K_2SO_4, respectively. The presence of Mg^{2+} had no detectable influence over the titration curve, indicating that interaction of this cation with $\mathbf{L}H_n^{n+}$ species is negligible. Sulfate, however, substantially perturbed the titration curve, suggesting some interactions with the ligand (Supporting Information). Modeling the equilibria with Hyperquad resulted in association constants (as logK) for 1:1 SO_4^{2-} binding by $\mathbf{L}H_4^{4+}$, $\mathbf{L}H_3^{3+}$, and $\mathbf{L}H_2^{2+}$ of 2.62(4), 2.45(4), and 1.8(1), respectively. On the other hand, no sulfate binding by $\mathbf{L}H^+$ or free **L** was apparent under these conditions. Furthermore, other plausible sulfate complexes of different stoichiometry, such as $SO_4(\mathbf{L}H_n)_2$, could not be detected. Concomitant addition of Mg^{2+} and SO_4^{2-} in the required stoichiometry for the formation of **1a** also did not have any measurable influence over the titration curve of LH_4^{4+} (up to the onset of precipitation of **1a**), suggesting that formation of $MgSO_4(\mathbf{L})_2$ capsules of the type observed in the crystalline state is negligible in water.

Figure 2 depicts the crystal structure of $\mathbf{L}H_4(SO_4)_2$. Protonation of the bridging tertiary N atom resulted in twisting of one of the urea groups so that its C═O group points inside the cavity to form an intramolecular NH···O hydrogen bond. As a result, only two urea groups remained available to bind sulfate via chelate hydrogen bonds along adjacent edges. The second sulfate links adjacent $\mathbf{L}H_4$ units in the crystal through hydrogen bonding with pyridinium donor groups. Water molecules included in the crystal (not shown) provide additional hydrogen bonding to the sulfate anions.

(18) *SHELXTL 6.12*; Bruker AXS, Inc.: Madison, WI, 1997.
(19) Martell, A. E.; Motekaitis, R. J. *Determination and Use of Stability Constants*, 2nd ed.; VCH Publishers: New York, 1992.

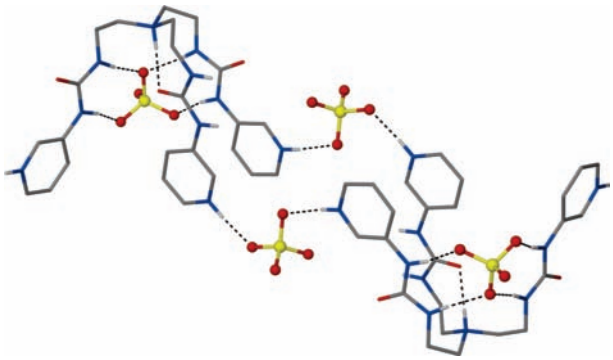

Figure 2. Crystal structure of $\mathbf{L}H_4(SO_4)_2$ showing hydrogen bonding of sulfate by urea and pyridinium groups.

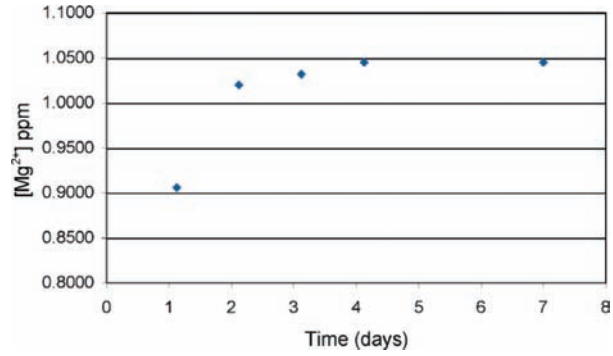

Figure 3. Kinetics of dissolution of **1a** in borax-buffered water at room temperature, measured by ICP.

Table 2. Measured Solubility Product of **1a** at 25 °C as a Function of Added Amounts of HNO_3

HNO_3 equiv	pH	K_{sp}(**1a**) × 10^{18} titration	K_{sp}(**1a**) × 10^{18} ICP
1	5.33	5.7	6.3
1.25	5.24	3.2	5.8
1.5	5.15	3.0	4.9
1.75	5.11	4.5	4.9
2	5.04	3.8	4.2
2.5	4.98	4.0	4.8
3	4.94	5.2	7.6

Determination of Solubility Products in Acidic Aqueous Solutions by Potentiometric Titrations. The dissolution of **1a** and its solubility product, K_{sp}, are defined according to eqs 1 and 2, respectively:

$$MgSO_4(\mathbf{L})_2(H_2O)_6 \rightleftarrows Mg^{2+} + SO_4^{2-} + 2\mathbf{L} + 6H_2O \quad (1)$$

$$K_{sp}(\mathbf{1a}) = (a_{Mg^{2+}})(a_{SO_4^{2-}})(a_L)^2 = \gamma_{Mg^{2+}}[Mg^{2+}]\gamma_{SO_4^{2-}}[SO_4^{2-}]\gamma_L^2[\mathbf{L}]^2 \quad (2)$$

The activity coefficients for the Mg^{2+} and SO_4^{2-} ions, $\gamma_{Mg}{}^{2+}$ and $\gamma_{SO4}{}^{2-}$, can be considered identical ($\gamma_{\pm}$) and estimated using the Debye−Hückel extended formula, whereas the activity coefficient of the neutral **L**, γ_L, can be considered equal to 1. Equation 2 thus becomes:

$$K_{sp}(\mathbf{1a}) = \gamma_{\pm}^2[Mg^{2+}][SO_4^{2-}][\mathbf{L}]^2 \quad (3)$$

By measuring the pH of saturated aqueous solutions of **1a** and the total amounts of dissolved $\mathbf{L}H_n{}^{n+}$ species through titration, [**L**] can be determined based on the previously determined equilibrium constants involving the ligand. The corresponding concentrations of Mg^{2+} and $SO_4{}^{2-}$ can then be simply derived from the known stoichiometry of **1a**, thereby allowing the calculation of K_{sp}(**1a**). The apparent solubility of **1a** increases at lower pH due to dissolution of **L** as $\mathbf{L}H_n{}^{n+}$. However, the measured solubility product should stay constant regardless of pH, provided the system is under thermodynamic equilibration. A relatively constant K_{sp}(**1a**) in the presence of increasing amounts of acid would confirm the validity of the invoked equilibria. Table 2 lists the obtained K_{sp} values measured for saturated solutions of **1a** in the presence of different amounts of HNO_3 (between 1 and 3 mol equiv). Also listed are the K_{sp} values obtained from the same solutions based on the Mg^{2+} concentrations measured independently by ICP. Evidently, the measured solubility products vary minimally within this pH range, and the two different methods provide consistent results, with corresponding average values for K_{sp}(**1a**) of $4.2 \pm 0.7 \times 10^{-18}$ and $5.5 \pm 0.8 \times 10^{-18}$ by titration or ICP, respectively.

Determination of Solubility Products in Alkaline Aqueous Solutions by ICP. Although the previous method proved suitable for determining the K_{sp} of **1a**, its application to the analogous carbonate and sulfite complexes (**1c**,**d**) is more problematic due to the required acidic conditions that may result in decomposition of these anions. Another problem is that the amount of free **L** is very small (<1% of total $\mathbf{L}H_n{}^{n+}$) in the pH range of the measurements, so the accurate determination of [**L**] is prone to systematic errors. We therefore sought a different approach amenable to neutral or slightly basic conditions. According to the previously established speciation and equilibrium constants of **L** in solution, at pH > 9 virtually all (>99%) dissolved ligand is unprotonated. Measurement of solubility products under such conditions is therefore simplified by eliminating the need to measure the exact pH of the solution. It is, however, important to maintain the pH below 10 to avoid the formation of $MgOH^+$ and $Mg(OH)_2$ species. The optimal basic conditions can be achieved through borax buffering, which regulates the pH around 9. Under such conditions, measuring the Mg^{2+} concentrations of saturated solutions of **1a**−**d** by ICP is sufficient to determine the corresponding K_{sp} values, as the concentrations of the anions and **L** are related to [Mg^{2+}] by the known stoichiometries of the complexes.

The kinetics of dissolution of **1a** were first measured to evaluate the amount of time required to reach equilibrium. As illustrated in Figure 3, the concentration of Mg^{2+} in the filtrate obtained from a mechanically stirred suspension of **1a** in water at room temperature steadily increases and reaches a plateau after 4 days. Allowing for an extra day as a margin of error, all subsequent measurements in this study were done on solutions equilibrated for 5 days.

To further ensure that the system behaves as a true equilibrium according to eq 2, saturated solutions of **1a** were prepared at 25 °C in the presence of increasing amounts of excess sulfate (added as K_2SO_4), and the resulting equilibrium Mg^{2+} concentrations were measured by ICP. As expected based on eq 3, as [$SO_4{}^{2-}$] increases, [Mg^{2+}] decreases, and the measured K_{sp} remains virtually constant up to about 80-fold excess sulfate (Table 3). An average value for K_{sp}(**1a**) of $2.0 \pm 0.3 \times 10^{-17}$ is obtained from these data. At higher sulfate concentrations, the obtained solubility product of **1a** starts to increase, possibly indicating the onset of other equilibria or an activity effect. We note here that the K_{sp}(**1a**) value obtained by this method differs from the earlier value obtained from acidic solutions by a factor

Table 3. Measured Solubility Product of **1a** in Borax-Buffered Water at 25 °C as a Function of Added Amounts of Sulfate[a]

SO_4^{2-} added (equiv)[b]	I (mol/L)[c]	γ[d]	$[Mg^{2+}] \times 10^5$ (mol/L)[e]	K_{sp}(**1a**) $\times 10^{17}$
0	0.016	0.61	5.86	**1.7**
10	0.018	0.59	2.97	**2.5**
20	0.020	0.58	2.30	**2.1**
30	0.022	0.57	1.75	**1.3**
40	0.023	0.56	1.74	**1.7**
50	0.025	0.55	1.73	**2.0**
80	0.031	0.52	1.62	**2.3**
100	0.035	0.50	1.94	4.7
500	0.098	0.37	2.29	21

[a] The values retained for the calculation of the average K_{sp} are in bold. [b] Molar equivalents of sulfate added to **1a**. [c] Ionic strength. [d] Activity coefficients from extended Debye−Hückel formula: $\log(\gamma) = -0.51z^2[(I^2)/(1 + 1.5I^2)]$. [e] Magnesium concentrations determined by ICP.

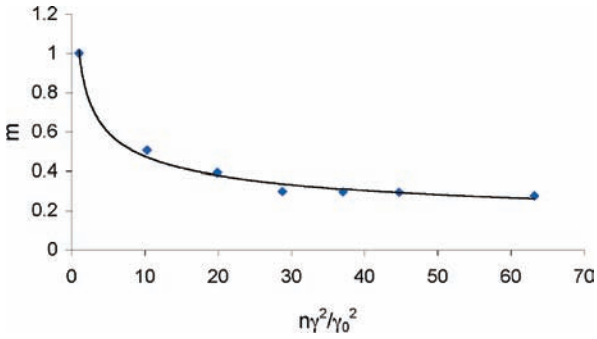

Figure 4. Observed interdependence between Mg^{2+} and SO_4^{2-} concentrations in saturated solutions of **1a** ($m = [Mg^{2+}]/[Mg^{2+}]_0$, $n = [SO_4^{2-}]/[SO_4^{2-}]_0$). The black curve was obtained by regression analysis of the data points (diamonds), and corresponds to the equation $y = 1.01x^{-0.33}$ ($R^2 = 0.98$).

of about 4. While the exact source of this discrepancy remains uncertain, the most likely factor is the introduction of systematic errors in the estimation of [**L**] from the potentiometric titrations, originating from the speciation model or pH measurements. For consistency and direct comparison with the similar K_{sp} values obtained for **1b** and **1c** (vide infra), only the latter value, which is deemed more reliable, will be considered hereafter in this work.

Another way to probe whether dissolution of **1a** is under thermodynamic equilibration is to plot the relative decrease in the Mg^{2+} concentration, $m = [Mg^{2+}]/[Mg^{2+}]_0$, versus the relative increase in the SO_4^{2-} concentration, $n = [SO_4^{2-}]/[SO_4^{2-}]_0$. According to eq 3, and considering that $[\mathbf{L}] = 2[Mg^{2+}]$, these quantities should be related by the following relationship:

$$m = [n(\gamma/\gamma_0)^2]^{-1/3} \quad (4)$$

Indeed, as Figure 4 shows, up to 80-fold excess sulfate, m decreases exponentially with $n(\gamma/\gamma_0)^2$, and the power regression analysis of the data points gives $y = 1.01x^{-0.33}$ ($R^2 = 0.98$), in excellent agreement with the theoretically expected eq 4.

Solubility products of the analogous SeO_4^{2-} (**1b**) and SO_3^{2-} (**1c**) complexes were subsequently determined by measuring the Mg^{2+} concentrations of the corresponding saturated solutions obtained from stirred suspensions of **1b**−**c** in borax-buffered water. The obtained K_{sp} values for **1b** and **1c** were $5.5 \pm 0.6 \times 10^{-16}$ and $6.6 \pm 0.3 \times 10^{-16}$, respectively. The carbonate complex **1d**, on the other hand, proved to be too soluble in pure water relative to **L** and solid $MgCO_3$, in contrast with the crystallization from H_2O/MeOH.[8e] Thus, at 25 °C, the solubilities of **1a**−**d** in water follow the order: **1a** < **1b** < **1c** < **1d**.

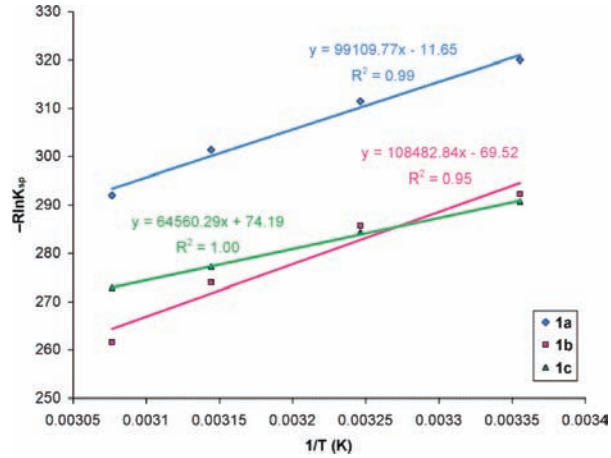

Figure 5. Van't Hoff plots for dissolution of **1a**−**c** at 25, 35, 45, and 52 °C.

Determination of $\Delta H°$ and $\Delta S°$ of Crystallization. Standard enthalpies and entropies of crystallization for **1a**−**c** were determined by measuring K_{sp} values at three additional temperatures: 35, 45, and 52 °C, and applying the van't Hoff equation:

$$\ln K_{sp} = -\Delta H°/RT + \Delta S°/R \quad (5)$$

Figure 5 shows the van't Hoff plots of $-R \ln K_{sp}$ against $1/T$ for **1a**−**c**, with the slopes and intercepts corresponding to $\Delta H°$ (J/mol) and $-\Delta S°$ (J/mol K) of dissolution, respectively.

Competitive Crystallizations. Having established the thermodynamics of crystallization for **1a**−**c**, we asked whether the obtained parameters are reflected in the selectivity observed in anion competition experiments. On the basis of the measured K_{sp} values, among the competing anions, we expected sulfate to be almost exclusively separated through crystallizations from aqueous solutions. However, preliminary results[8e] indicated that selenate was also included in substantial amounts ($SO_4^{2-}/SeO_4^{2-} = 3$) in the crystalline complexes precipitated from mixed solutions in H_2O/MeOH 1:1 (v/v). To assess the influence of the solvent and pH, a competitive crystallization from an equimolar mixture of SO_4^{2-}, SeO_4^{2-}, SO_3^{2-}, and CO_3^{2-} was performed in borax-buffered water (Exp *A*) for direct comparison with the measured solubility products. In this experiment, the initial ratio of Mg^{2+}, **L**, and divalent anion was 1:2:1, a condition that would thermodynamically allow the least soluble crystals (i.e., **1a**) to form exclusively. The FTIR spectrum of the precipitated solid after 5 days (Figure 6a), however, showed that sulfate and selenate crystallized in similar proportions as in the analogous crystallization from H_2O/MeOH, whereas the amounts of the other two anions in the solid were below detection limits for this method. Thus, sulfate and selenate are selectively coseparated from either water or water/methanol solvents.

The next question was whether these competitive crystallizations reached thermodynamic equilibrium, or the observed selectivity was mainly determined by kinetics. To answer this question, three additional competition experiments between SO_4^{2-} and SeO_4^{2-} were performed. In the first experiment (*B*), sulfate and selenate were both added initially to the aqueous mixture, thereby allowing their concomitant precipitation. In the second experiment (*C*), only sulfate was initially added, resulting in precipitation of **1a**, followed by addition of selenate.

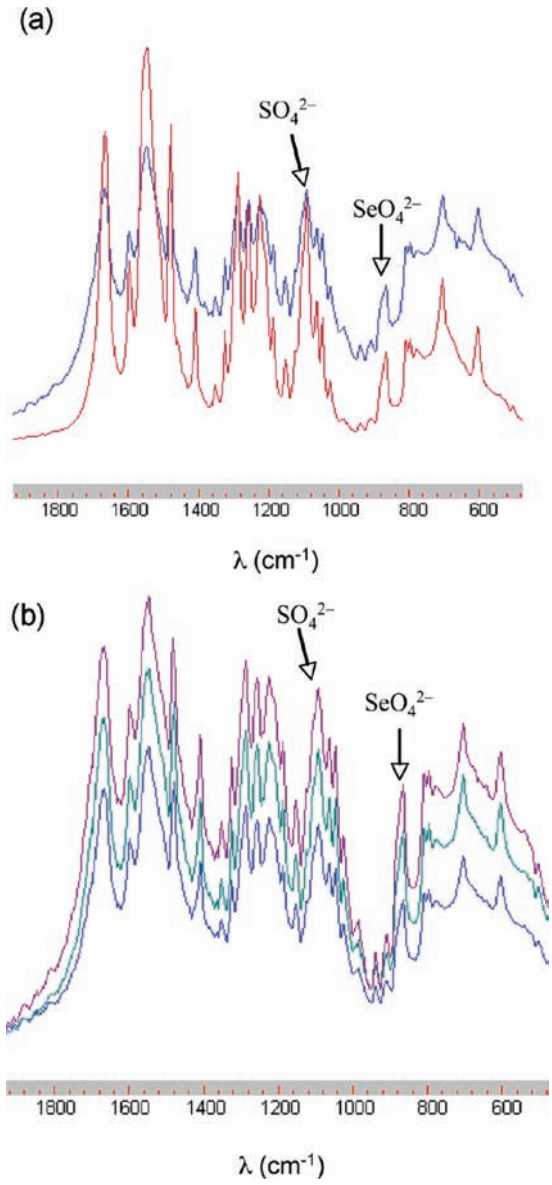

Figure 6. (a) FTIR spectra of the crystalline solids obtained from competitive crystallizations in borax-buffered water (Exp *A*) and H_2O/MeOH 1:1,[8e] shown in blue and red, respectively. (b) FTIR spectra of the crystalline solids obtained from competitive crystallizations of sulfate and selenate from borax-buffered aqueous solutions. Purple: SO_4^{2-} and SeO_4^{2-} added simultaneously (Exp *B*); Green: **1a** + SeO_4^{2-} (Exp *C*); Blue: **1b** + SO_4^{2-} (exp *D*). The spectra were scaled differently to minimize overlap and enhance clarity.

Finally, in the last experiment (*D*), **1b** was initially precipitated, followed by addition of sulfate. All solids were collected after 5 days and analyzed by FTIR and elemental analysis. The relative molar amounts of sulfate and selenate in the three crystalline solids were found to be very similar by both infrared spectroscopy (Figure 6b), and elemental analysis (SO_4^{2-}/SeO_4^{2-} = 2.7 ± 0.3), strongly indicating that the equilibrium point had been reached.

Single-crystal X-ray diffraction experiments confirmed that SO_4^{2-} and SeO_4^{2-} prefer to form solid solutions rather than crystallize separately as **1a** and **1b**. Thus, crystals grown by H_2O/MeOH layering from equimolar mixtures of sulfate and selenate were substitutionally disordered with both anions occupying the same sites in the crystals (Table 1). Not surprisingly, thermodynamic equilibration is significantly retarded under the slow diffusion conditions required for growing large single crystals (as opposed to the fast stirring conditions in Exp *A*−*D*, which resulted in fine precipitates). Thus, the single crystals initially isolated after 5 days contained 35% sulfate and 65% selenate. The sulfate content in the crystals increases very slowly toward the equilibrium value of 73%, reaching 52% after 33 days, and 57% after 67 days. Inclusion of selenate appears to be kinetically favored, possibly due to the lower energy required for its dehydration.[22]

Discussion

The $\mathbf{L}H_n^{n+}$ (n = 2−4) protonated forms of the tripodal ligand **L** bind sulfate in water with 1:1 log K association constants of 1.8 (n = 2), 2.45 (n = 3), and 2.62 (n = 4). These constants are comparable with those of sulfate binding in water by the parent tren ligand, for which the corresponding log K values for mono-, di-, and triprotonated forms were found to be 1.66, 1.72, and 2.22, respectively.[12] This indicates that similar to protonated tren, anion binding by $\mathbf{L}H_n^{n+}$ is dominated by electrostatic interactions. As a result, the unprotonated **L** or even the monoprotonated $\mathbf{L}H^+$ do not bind sulfate to any substantial extent in this competitive medium. In addition to Coulombic interactions, hydrogen bonding by the urea and pyridinium groups are also likely to contribute to sulfate binding, as suggested by the crystal structure of $\mathbf{L}H_4(SO_4)_2$ (Figure 2). However, due to the high flexibility of the tren structure and the significant exposure of the anions to water solvent, poor discrimination among anions of same charge is expected from such relatively simple protonated tripodal receptors.

The situation is drastically different in the crystalline **1a**−**d** complexes, where the anions are completely sequestered from the water molecules into well-defined and rigid hydrogen-bonded capsules assembled with the help of $Mg(H_2O)_6^{2+}$ cations. Six urea groups from two **L** molecules provide 12 stabilizing hydrogen bonds to each encapsulated anion, which are most complementary to tetrahedral SO_4^{2-} and SeO_4^{2-} oxoanions.[16] The pyramidal SO_3^{2-} and trigonal-planar CO_3^{2-} anions, on the other hand, engage in repulsive NH···S and NH···C interactions, which are expected to lower their binding energy. Monoanions like NO_3^-, ClO_4^-, F^-, Cl^-, Br^-, and I^- are completely excluded due to their charge mismatch relative to the $Mg(H_2O)_6^{2+}$ cation.[8e] Equally important to selectivity is the rigidity of the crystalline framework, which does not distort to avoid these repulsive interactions and thereby reoptimize the binding of competing anions. Another important consequence of framework's rigidity is that all anions form isomorphous structures, thereby simplifying the interpretation of the observed selectivity based on differences in anion coordination geometries.

Table 4 summarizes the thermodynamic parameters obtained for crystallization of **1a**−**c** in borax-buffered aqueous solutions. The corresponding parameters for **1d** could not be obtained due to the high solubility of this compound in water relative to **L** and $MgCO_3$, which crystallized instead. The sulfate complex **1a** is the least soluble, and the measured K_{sp} values for the selenate and sulfite analogs are 27.5 and 33 times higher, respectively. This is different from the Hofmeister order, which would predict the selenate complex **1b** to be the least soluble based on its lower energy cost of dehydration.

In each case, crystallization is enthalpy driven, in contrast with anion binding by protonated tren derivatives in water, which is typically controlled by entropy. However, direct comparison between such disparate processes needs to be done with caution, as in addition to dehydration of the anion and **L**,

Table 4. Thermodynamic Parameters for Crystallization of **1a**−**c** in Borax-Buffered Water

complex	K_{sp}	ΔG°_{cryst} (kJ/mol)	ΔH°_{cryst} (kJ/mol)	$T\Delta S^{\circ}_{cryst}$ (kJ/mol)[a]
1a	$2.0 \pm 0.3 \times 10^{-17}$	-95.3 ± 0.4	-99.1 ± 1.9	-3.8 ± 2.3
1b	$5.5 \pm 0.6 \times 10^{-16}$	-87.1 ± 0.3	-108.5 ± 2.3	-21.4 ± 2.6
1c	$6.6 \pm 0.3 \times 10^{-16}$	-86.6 ± 0.1	-64.6 ± 0.8	22.0 ± 0.9

[a] $T\Delta S^{\circ}_{cryst}$ values and the corresponding uncertainties were calculated using: $\Delta G^{\circ}_{cryst} = \Delta H^{\circ}_{cryst} - T\Delta S^{\circ}_{cryst}$.

and the anion-binding interactions, crystallization of **1a**−**c** involves cation dehydration, ion pairing, and crystal packing phenomena. More meaningful here is the comparison with crystallizations of MgX salts (X = SO_4^{2-}, SeO_4^{2-}, SO_3^{2-}, CO_3^{2-}), which are endothermic and entropy driven.[20] The relative solubilities of **1a**−**d** (**1a** < **1b** < **1c** < **1d**) are also in direct contrast to those of the simple MgX salts ($MgCO_3$ < $MgSO_3$ < $MgSO_4$), which simply follow the increase in the anion radii. One major factor that apparently makes the difference in **1a**−**d** is the anion recognition through encapsulation into the urea-functionalized cavities, which evidently favors the tetrahedral SO_4^{2-} and SeO_4^{2-} anions. The most favorable enthalpy of crystallization corresponds to SeO_4^{2-}, which may indicate the best size and shape complementarity between this anion and the urea-lined cavities of the hydrogen-bonding capsules. Overall though, sulfate is favored due to its less negative entropy of crystallization, presumably a combined result of more favorable dehydration entropy and less tight binding in the crystalline capsules. Sulfite, on the other hand, has the least favorable enthalpy of crystallization, which may be correlated with its noncomplementary shape and size relative to the capsules' cavities. This is however largely compensated by its highly favorable entropy of crystallization,[21] resulting in a ΔG°_{cryst} almost identical to that of the selenate complex. Thus, besides shape complementarity, entropy plays an important role in the observed selectivity.[10]

To gain further insight into anion inclusion selectivity in this series of crystalline capsules, their free energy of crystallization can be broken down into two components: dehydration of the molecular and ionic constituents ($-\Delta G^{\circ}_{h}$), and gas-phase crystal lattice formation (ΔG°_{latt}), according to eq 6:

$$\Delta G^{o}_{cryst} = \Delta G^{o}_{latt} - \Delta G^{o}_{h} \quad (6)$$

The $-\Delta G^{\circ}_{h}$ term encompasses the dehydration of all components: the ligand **L**, the anion (−), and the cation (+). In a competitive setting, where each competing framework contains the same ligand and cation, their dehydration energies cancel out, and therefore:

$$\Delta\Delta G^{o}_{cryst} = \Delta\Delta G^{o}_{latt} - \Delta\Delta G^{o}_{h}(-) \quad (7)$$

The relative free energies of crystallization are thus given by the relative gas-phase stabilities of the competing crystalline frameworks and the relative anion hydration energies. In the case of SeO_4^{2-}, SO_4^{2-}, and SO_3^{2-}, the corresponding $-\Delta G^{\circ}_{h}$ values are 900, 1080, and 1295 kJ/mol, respectively.[22] Using the ΔG°_{cryst} values measured in this study and listed in Table 4, the relative gas-phase stability of **1a**−**c** ($\Delta\Delta G^{\circ}_{latt}$, kJ/mol) can be calculated: **1b** (0) < **1a** (−188) < **1c** (−395). Thus, like ΔG°_{h}, ΔG°_{latt} follows the same trend: it increases (becomes more negative) with the decrease in the anion radii. In other words, sulfite, the anion with the highest charge density, will form the most stable crystal lattice from the gas phase.[23] It becomes thus revealing that $\Delta\Delta G^{\circ}_{cryst}$, which defines the upper limits of anion selectivities achievable in this series, is a relatively small quantity resulting from adding up two large energies of opposite signs. Despite the apparent monotonous trends of ΔG°_{h} and ΔG°_{latt}, peak selectivity for sulfate is nevertheless observed. Can then shape recognition still be invoked to explain the observed selectivity? To answer this question, one can analyze the case of SO_3^{2-}. Because of its highest charge density, it interacts strongest with any hydrogen-bonding environment, be that water or the crystalline capsules. There is, however, an energetic penalty associated with transferring sulfite from the water solvent that can freely rearrange to optimize the anion binding, to the rigid and much more structured space inside the hydrogen-bonding capsule, which is not optimal for accommodating its pyramidal shape. In contrast, there is no such penalty for the tetrahedral sulfate and selenate, which can compensate for their lower hydrogen-bond accepting abilities with better complementarity to the binding site. As a result, the stabilization of these anions upon transferring from water into the crystalline capsules is greater than for the misshaped sulfite.

Despite the lower solubility of **1a** versus **1b**, cocrystallization of sulfate and selenate was observed in the competitive crystallizations. On the basis of the K_{sp} values obtained for **1a**−**c**, one would expect sulfate to be selectively separated by a significant margin over the other three anions in a competitive setting from an equimolar mixtures of SO_4^{2-}, SeO_4^{2-}, SO_3^{2-}, and CO_3^{2-}. However, while the competitive crystallization resulted in virtually complete exclusion of sulfite and carbonate, both sulfate and selenate were present in the crystallized solid in a ratio of 2.7:1. This selectivity is significantly lower than predicted by the K_{sp} values of **1a** and **1b**. Single-crystal X-ray diffraction analysis of the crystals obtained from 1:1 SO_4^{2-}/SeO_4^{2-} aqueous mixtures indicated that these tetrahedral anions have a propensity to crystallize together into solid solutions. The explanation for this behavior is their very similar size and shape, which translates into almost identical crystal structures for **1a** and **1b**. The two compounds in fact satisfy all Kitaigorodsky's conditions for the formation of mixed crystals with unlimited solubility: same space group, close unit cell dimensions (<1% difference), similar molecular shape, crystal packing, and hydrogen-bonding interactions.[24] In more quantitative terms, the free energy of crystallization of a binary solid solution (ΔG°_{ss}) from the pure components A and B is given by eq 8:[24]

(20) Wagman, D. D.; Evans, W. H.; Parker, V. B.; Schumm, R. H.; Halow, I.; Bailey, S. M.; Churney, K. L.; Nuttal, R. L.; *J. Phys. Chem. Ref. Data* **1982**, *11*, Suppl. No. 1.

(21) The crystal structure of **1c** showed that SO_3^{2-} is 6-fold disordered inside the capsule, compared to the 3-fold disorder of SO_4^{2-} and SeO_4^{2-} in **1a** and **1b**.[8e] This likely contributes to the more favorable entropy of crystallization of **1c**.

(22) Marcus, Y. *J. Chem. Soc. Faraday Trans.* **1991**, *87*, 2995.

(23) This trend is similar to that observed in binding of alkali metal cations by crown ethers in the gas phase, which is directly proportional to the cation's charge density (i.e., the highest affinity is observed for Li^+, regardless of the size of the crown ether). Schneider, H. J.; Yatsimirsky, A. K. *Chem. Soc. Rev.* **2008**, *37*, 263.

(24) Kitaigorodsky, A. I. *Mixed Crystals*; Springer-Verlag: Berlin, Heidelberg, New York, Tokyo, 1984.

$$\Delta G^{o}_{ss} = (1 - x)\Delta G^{o}_{A} + x\Delta G^{o}_{B} + \Delta G^{o}_{mix} \quad (8)$$

ΔG°_{A} and ΔG°_{B} are the free energies of crystallization of the pure components, x is the molar fraction of B in the mixed crystal, and ΔG°_{mix} is the free energy of mixing, which must be a negative quantity for the solid solution to form. In the current case, using the measured ΔG°_{cryst} values for SO_4^{2-} and SeO_4^{2-} listed in Table 4, and the observed $x = 0.27$ for selenate, results in $\Delta G^{\circ}_{ss} = -93.1 + \Delta G^{\circ}_{mix}$. For the solid solution to form, ΔG°_{ss} needs to be more negative than -95.3 kJ mol^{-1}, the corresponding value of ΔG°_{cryst} for the pure sulfate crystal. It thus follows that ΔG°_{mix} must be more negative than -2.2 kJ mol^{-1}. Formation of crystalline solid solutions is typically accompanied by an increase in entropy ($\Delta S^{\circ}_{mix} > 0$), with the configurational entropy term, $\Delta S^{\circ}_{config}$, often making a dominant contribution to ΔS°_{mix}.[24] This entropy component is given by eq 9:

$$\Delta S^{o}_{config} = -R[(1 - x)\ln(1 - x) + x \ln x] \quad (9)$$

In the present case, $T\Delta S^{\circ}_{config} = -1.4$ kJ mol^{-1}, which accounts for much of the -2.2 kJ mol^{-1} minimum value of $\Delta G^{\circ}_{config}$ required for the formation of the observed solid solution.

Conclusions

Crystallization of hydrogen-bonding capsules represents an effective new approach to selective anion separation from competitive aqueous environments. Like in traditional molecular receptors, functionalization with complementary hydrogen-bonding groups and complete anion sequestration from the surrounding water solvent appear to be prerequisites for high selectivity. Equally important is the organizational rigidity of the crystalline framework, which is necessary to prevent structural rearrangements and accommodation of competing anions. In this respect, crystalline capsules may have an edge over discrete molecular analogues in solution, thanks to the stiffer environment typically associated with a crystal lattice. In the present system, anion encapsulation into rigid and highly complementary urea-functionalized crystalline capsules resulted in shape selectivity for the tetrahedral sulfate and selenate oxoanions against the pyramidal sulfite and trigonal-planar carbonate. Extensive thermodynamic measurements indicated that these hydrogen-bonded capsules do not persist in aqueous solutions. K_{sp} measurements established that the sulfate-containing crystalline capsules have the lowest aqueous solubility, followed by the selenate and sulfite analogues, whereas the carbonate analogue proved unstable in water. Crystallization of these crystalline capsules is enthalpy driven, with selenate displaying the most negative enthalpy of crystallization, closely followed by sulfate, in agreement with the X-ray structural data suggesting shape complementarity for these tetrahedral anions. By comparison, sulfite has a considerably less exothermic enthalpy of crystallization, apparently due to its poor fit inside the urea-functionalized capsules. Entropy, however, has a compensation effect, strongly favoring sulfite over selenate and sulfate. The selectivity observed in competitive crystallizations is consistent with the measured thermodynamic parameters, except for the inclusion of larger amounts of selenate than predicted by the K_{sp} values alone, a result of the propensity of sulfate and selenate to form solid solutions. Formation of solid solutions thus appears to be a potentially limiting factor determining selectivity in the separation of anions with similar shape and size by competitive crystallizations.

The exceptional selectivity observed in crystallization of Mg^{2+}, **L**, and divalent oxoanions suggests practical applications. Among a variety of univalent and divalent anions, the sulfate-selenate selectivity appears to be the only obvious limitation, which seems to us remarkable. In fact, it is possible to envision practical applications in industrial separations of either of these anions. For example, sulfate and selenate contamination of groundwater represent environmental challenges,[25] and sulfate represents a problem constituent of legacy nuclear waste, which is otherwise difficult to vitrify owing to the low solubility of this anion in borosilicate glass.[26] Accordingly, the crystallization of **1a** and **1b** and even their solid solutions presents possibilities for industrial applications of considerable significance.

Acknowledgment. This research was sponsored by the Division of Chemical Sciences, Geosciences, and Biosciences, Office of Basic Energy Sciences, U.S. Department of Energy.

Supporting Information Available: Hyperquad plots and X-ray crystallographic data (CIF). This material is available free of charge via the Internet at http://pubs.acs.org.

JA101354R

(25) (a) Hunter, W. J. *Curr. Microbiol.* **2006**, *53*, 244. (b) Jegadeesan, G.; Mondal, K.; Lalvani, S. B. *Environ. Technol.* **2005**, *26*, 1181. (c) Haghsheno, R.; Mohebbi, A.; Hashemipour, H.; Sarrafi, A. *J. Hazard. Mater.* **2009**, *166*, 961. (d) Darbi, A.; Viraraghavan, T.; Jin, Y. C.; Braul, L.; Corkal, D. *Water Qual. Res. J. Can.* **2003**, *38*, 169.

(26) Moyer, B. A.; Delmau, L. H.; Fowler, C. J.; Ruas, A.; Bostick, D. A.; Sessler, J. L.; Katayev, E.; Pantos, G. D.; Llinares, J. M.; Hossain, M. A.; Kang, S. O.; Bowman-James, K. *Adv. Inorg. Chem.* **2007**, *59*, 177.